Striatal Pre- and Postsynaptic Profile of Adenosine A$_{2A}$ Receptor Antagonists

Marco Orru[1], Jana Bakešová[2], Marc Brugarolas[2], César Quiroz[1], Vahri Beaumont[3], Steven R. Goldberg[1], Carme Lluís[2], Antoni Cortés[2], Rafael Franco[2], Vicent Casadó[2], Enric I. Canela[2], Sergi Ferré[1]*

1 National Institute on Drug Abuse, IRP, NIH, DHHS, Baltimore, Maryland, United States of America, 2 Centro de Investigación Biomédica en Red sobre Enfermedades Neurodegenerativas (CIBERNED), Faculty of Biology, University of Barcelona, Barcelona, Spain, 3 CHDI Management, CHDI Foundation, Los Angeles, California, United States of America

Abstract

Striatal adenosine A$_{2A}$ receptors (A$_{2A}$Rs) are highly expressed in medium spiny neurons (MSNs) of the indirect efferent pathway, where they heteromerize with dopamine D$_2$ receptors (D$_2$Rs). A$_{2A}$Rs are also localized presynaptically in cortico-striatal glutamatergic terminals contacting MSNs of the direct efferent pathway, where they heteromerize with adenosine A$_1$ receptors (A$_1$Rs). It has been hypothesized that postsynaptic A$_{2A}$R antagonists should be useful in Parkinson's disease, while presynaptic A$_{2A}$R antagonists could be beneficial in dyskinetic disorders, such as Huntington's disease, obsessive-compulsive disorders and drug addiction. The aim or this work was to determine whether selective A$_{2A}$R antagonists may be subdivided according to a preferential pre- versus postsynaptic mechanism of action. The potency at blocking the motor output and striatal glutamate release induced by cortical electrical stimulation and the potency at inducing locomotor activation were used as in vivo measures of pre- and postsynaptic activities, respectively. SCH-442416 and KW-6002 showed a significant preferential pre- and postsynaptic profile, respectively, while the other tested compounds (MSX-2, SCH-420814, ZM-241385 and SCH-58261) showed no clear preference. Radioligand-binding experiments were performed in cells expressing A$_{2A}$R-D$_2$R and A$_1$R-A$_{2A}$R heteromers to determine possible differences in the affinity of these compounds for different A$_{2A}$R heteromers. Heteromerization played a key role in the presynaptic profile of SCH-442416, since it bound with much less affinity to A$_{2A}$R when co-expressed with D$_2$R than with A$_1$R. KW-6002 showed the best relative affinity for A$_{2A}$R co-expressed with D$_2$R than co-expressed with A$_1$R, which can at least partially explain the postsynaptic profile of this compound. Also, the in vitro pharmacological profile of MSX-2, SCH-420814, ZM-241385 and SCH-58261 was is in accordance with their mixed pre- and postsynaptic profile. On the basis of their preferential pre- versus postsynaptic actions, SCH-442416 and KW-6002 may be used as lead compounds to obtain more effective antidyskinetic and antiparkinsonian compounds, respectively.

Introduction

The striatum is the major input structure of the basal ganglia [1]. More than ninety five percent of striatal neurons are γ-aminobutyric-acidergic (GABAergic) medium spiny neurons (MSNs). These neurons receive two main inputs: glutamatergic afferents from cortical, thalamic and limbic areas and dopaminergic afferents from the substantia nigra pars compacta and the ventral tegmental area [1]. MSNs are efferent neurons that give rise to the two efferent pathways of the basal ganglia, the 'direct' and 'indirect' striatal efferent pathways [1]. It is generally accepted that stimulation of the direct and indirect pathways results in motor activation and motor inhibition, respectively, and that smooth motor drive results from the counterbalanced influence of the direct and indirect pathways on the neural activity of the output structures [2,3]. Direct MSNs express

dopamine receptors predominantly of the D$_1$ receptor (D$_1$R) subtype, whereas indirect MSNs are known for their high expression of dopamine D$_2$ receptors (D$_2$Rs) and adenosine A$_{2A}$ receptors (A$_{2A}$Rs) [1,4,5].

There is clear evidence for the existence of postsynaptic mechanisms in the control of glutamatergic neurotransmission to the indirect MSN by at least two reciprocal antagonistic interactions between A$_{2A}$R and D$_2$R [4]. In one type of interaction, A$_{2A}$R and D$_2$R are forming heteromers and, by means of an allosteric interaction, A$_{2A}$R counteracts the D$_2$R-mediated inhibitory modulation of the effects of NMDA receptor stimulation in the indirect MSN, which includes Ca^{2+} influx, transition to the up-state and neuronal firing in the up-state [6,7]. This interaction has been suggested to be mostly responsible for the locomotor depressant and activating effects of A$_{2A}$R agonist and antagonists, respectively [4]. The second type of interaction

involves A$_{2A}$R and D$_2$R that do not form heteromers, but most probably homomers [4]. In this interaction, which takes place at the level of adenylyl-cyclase (AC), stimulation of G$_i$-coupled D$_2$R counteracts the effects of G$_{olf}$-coupled A$_{2A}$R [4]. Due to a strong tonic effect of endogenous dopamine on striatal D$_2$R, this interaction keeps A$_{2A}$R from signaling through AC. However, under conditions of dopamine depletion or with blockade of D$_2$R, A$_{2A}$R-mediated AC activation is unleashed. This is biochemically associated with a significant increase in the phosphorylation of PKA-dependent substrates, which increases gene expression and the activity of the indirect MSN, producing locomotor depression (reviewed in ref. [4]). This interaction seems to be the main mechanism responsible for the locomotor depression induced by D$_2$R antagonists. Thus the motor depressant and most biochemical effects induced by genetic or pharmacologic blockade of D$_2$R are counteracted by the genetic or pharmacological blockade of A$_{2A}$R [8–10].

Striatal A$_{2A}$Rs are not only localized postsynaptically but also presynaptically, in glutamatergic terminals, where they heteromerize with A$_1$ receptors (A$_1$Rs) and where their stimulation facilitates glutamatergic neurotransmission [5,11]. Interestingly, presynaptic A$_{2A}$Rs are preferentially localized in glutamatergic terminals of cortico-striatal afferents to the direct MSN [5]. According to the widely accepted functional basal circuitry model [2,3], blockade of postsynaptic A$_{2A}$R localized in the indirect MSN should produce motor activation (by potentiating D$_2$R-mediated effects by means of A$_{2A}$R-D$_2$R receptor interactions). On the other hand, according to the same model, blockade of presynaptic A$_{2A}$R localized in the cortico-striatal glutamatergic terminals that make synaptic contact with the direct MSN should decrease motor activity (by inhibiting glutamate release). The preferential locomotor-activating effects of systemically administered A$_{2A}$R receptor antagonists can be explained by a stronger influence of a tonic adenosine and A$_{2A}$R receptor-mediated modulation of the indirect pathway *versus* the direct pathway under basal conditions. In any case, the potency at inducing locomotor activation can be used as an *in vivo* measure of the ability of an A$_{2A}$R antagonist to block postsynaptic striatal A$_{2A}$R. Recently we have established an *in vivo* model that evaluates the efficacy of cortico-striatal glutamatergic neurotransmission to the direct MSN, by quantifying the correlation between the current delivered into the orofacial premotor cortex and the concomitant electromyographic response elicited in the jaw muscles [5]. In this model, A$_{2A}$R or D$_1$R antagonists were able to counteract the motor output induced by cortical electrical stimulation, which can only be explained by blockade of striatal presynaptic A$_{2A}$R or postsynaptic D$_1$R, respectively [5,12].

Receptor heteromer is defined as a macromolecular complex composed by at least two (functional) receptor units with biochemical properties that are demonstrably different from those of its individual components [13]. Specific ligand binding characteristics are one of those properties [13,14]. The aim of the present study was, first, to investigate the possible existence of different pre- and postsynaptic profiles of several A$_{2A}$R antagonists. The potency at blocking the motor output and striatal glutamate release induced by cortical electrical stimulation and the potency at inducing locomotor activation were used as *in vivo* measures of pre- and postsynaptic activities, respectively. Second, we wanted to evaluate if the different pre- and postsynaptic profiles could be related to different affinities that A$_{2A}$R could have for those compounds when forming heteromers with either A$_1$R or D$_2$R. In fact, the results strongly suggest that heteromerization plays a key role in the pre- and postsynaptic profile of A$_{2A}$R antagonists.

Materials and Methods

Ethics Statement

All animals used in the study were handled in accordance with the National Institutes of Health Animal care guidelines. The animal research conducted to perform this study was approved by the NIDA IRP Animal Care and Use Committee (under the auspices of protocol 09-BNRB-73) on 12/7/2009.

Animals

Male Sprague-Dawley rats (Charles River Laboratories, Wilmington, MA) weighting between 300–350 g were used in these experiments. Rats were housed 2 per cage and they maintained at a temperature of $22\pm2°C$ on a regular 12-h light–dark cycle. Food and water were available *ad libitum*.

Adenosine A$_{2A}$R antagonists

The following A$_{2A}$R antagonists were used: 2-(2-Furanyl)-7-[3-(4-methoxyphenyl)propyl]-7H-pyrazolo[4,3-e][1,2,4]triazolo[1,5-c]pyrimidin-5-amine (**SCH-442416**), 2-(2-Furanyl)-7-(2-phenylethyl)-7H-pyrazolo[4,3-e][1,2,4]triazolo[1,5-c]pyrimidin-5-amine (**SCH-58261**), 2-(2-furanyl)-7-[2-[4-[4-(2-methoxyethoxy)phenyl]-1-piperazinyl]ethyl]-7H-pyrazolo[4,3-e][1,2,4]-triazolo[1,5-c]pyrimidin-5-amine (**SCH-420814**), 4-(2-[7-Amino-2-(2-furyl)[1,2,4]triazolo[2,3-a][1,3,5]triazin-5-ylamino]ethyl)phenol (**ZM-241385**), (E)-1, 3-diethyl-8-(3,4-dimethoxystyryl)-7-methyl-3,7-dihydro-1H-purine-2,6-dione (**KW-6002**), (E)-3-(3-hydroxypropyl)-8-[2-(3-methoxyphenyl)vinyl]-7-methyl-1-prop-2-ynyl-3,7-dihydropurine-2,6-dione (**MSX-2**) and its water-soluble phosphate prodrug (E)-phosphoric acid mono-(3-{8-[2-(3-methoxyphenyl)vinyl]-7-methyl-2,6-dioxo-1-prop-2-ynyl-1,2,6,7-tetra-hydropurin-3-yl}propyl) ester disodium salt (MSX-3). **MSX-3** is a water-soluble phosphate pro-drug of MSX-2; in vivo MSX-3 is readily converted to the A$_{2A}$R antagonist MSX-2 (Sauer et al., 2002). For their systemic administration, the compounds were prepared as follows:

SCH-442416 and SCH 58261 were suspended in a solution of 5% dimethyl- sulfoxide (DMSO) (Sigma-Aldrich, St. Louis,MI), 5% TWEEN80 (Sigma-Aldrich, St. Louis, MI) and 90% ddH$_2$O; SCH-420814 was suspended in a solution of 20% PEG400, 40% β-cyclodextrin and 40% Lutrol 1% (in ddH$_2$O); ZM-241385 was suspended in a solution of 15% DMSO, 10% TWEEN80 and 75% ddH$_2$O; KW-6002 was suspended in a solution of 8% TWEEN80 and 92% ddH$_2$O; MSX-3 was dissolved in sterile saline (with 3 μl/ml saline of 1 M NaOH solution, final pH 7.4). All drugs but MSX-3 (Sigma-Aldrich, St. Louis, MI) were provided by CHDI Foundation Inc. (Los Angeles, CA, US). SCH-420814 was administered subcutaneously (s.c.) at 1 ml/kg and the other drugs were administered via intraperitonal (i.p.) injection at volume of 2 ml/kg.

Locomotor Activity

Locomotor activity was measured by placing the animals individually in motility soundproof chambers (50×50 centimeters; Med Associates Inc., VT). Locomotion was measured by counting the number of breaks in the infrared beams of the chambers. The animals were placed in individual acrylic chambers at noon on the day of testing. A lamp inside each chamber remained lit during this period. Following 90 min of habituation, the rats were injected i.p. with different doses of each compound or vehicle and locomotor activity was recorded for 90 min after the drug or vehicle administration. All the animals were tested only once. The effect of different doses of the A$_{2A}$R antagonists on locomotor activity were analyzed using a one-way analysis of variance (ANOVA), followed by Newman-Keuls' *post-hoc* test.

Surgical procedures

Rats were anesthetized with 3 ml/kg of Equithesin (4.44 g of chloral hydrate, 0.972 g of Na pentobarbital, 2.124 g of MgSO$_4$, 44.4 ml of propylene glycol, 12 ml of ethanol and distilled H$_2$O up to 100 ml of final solution; NIDA Pharmacy, Baltimore, MD) and implanted unilaterally with bipolar stainless steel electrodes, 0.15 mm in diameter (Plastics One, Roanoke, VA), into the orofacial area of the lateral agranular motor cortex (3 mm anterior, 3 and 4 mm lateral, and 4.2 mm below bregma). The electrodes and a head holder (connected to a swivel during stimulation) were fixed on the skull with stainless steel screws and dental acrylic resin. For the experiments with electromyographic (EMG) recording, electrodes were also implanted in mastication muscles (during the same surgical procedure). Two 5 mm-long incisions were made in the skin on the upper and lower jaw areas to expose the masseter and the lateral pterygoid muscles. Two silicon rubber-coated coiled stainless steel recording electrodes (Plastics One, Roanoke, VA) were slipped below the skin from the incision in the skull until the tips showed up from the incisions in the jaw. The bare tips of the electrodes were then held in contact with the masseter and the lateral pterygoid muscles and the skin was closed with surgical staples. The other end of the recording electrodes was encased in a molded plastic pedestal with a round threaded post which was attached to an electrical swivel and then to a differential amplifier (Grass LP511, Grass Instruments, Warwick, RI). The pedestal was secured to the skull with dental cement together with the stimulation electrodes. For the *in vivo* microdialysis experiments, concentric microdialysis probes with 2-mm long dialysis membranes (Eicom Corp., Tokio, Japan) were implanted respectively into the striatum ipsilateral to the stimulation electrodes (0.0 mm AP, 4.5 ML and 7.0 mm DV).

EMG recording and power correlation analysis

Rats were placed in individual bowl chambers. Both stimulation electrodes and recording electrodes were attached using flexible shielded cabling to a four channel electrical swivel. Stimulation electrodes were connected to two-coupled constant current isolation units (PSIU6X, Grass Instruments West Warwick, RI) driven by an electrical stimulator (Grass S88X; Grass Instruments). The recording electrodes were connected to a differential amplifier (Grass LP511, West Warwick, RI). This configuration allows the rat to move freely while the stimulation and EMG recordings are taking place. After 60 min of habituation, biphasic current pulse trains (pulse of 0.1 ms at 120–200 µA; 100 Hz, 160 ms trains repeating once per 2 seconds) were delivered. The current intensity was adjusted to the threshold level, defined as the minimal level of current intensity allowing at least 95% of the stimulation pulses to elicit a positive EMG response. Positive EMG response was defined as at least 100% increase of the peak to peak amplitude respect to the background tonic EMG activity lasting more than 100 ms or at least 70% increase in the power of the EMG signal respect to the baseline. Positive EMG responses always matched observable small jaw movements. The threshold level was different for each animal but it was very stable and reproducible once established. The threshold level was in the 100 to 150 µA range for most cases and it reached 200 µA in a few (6) animals. Animals that failed to show a positive EMG response with electrical cortical stimulation intensities of 200 µA were discarded from the experimental procedure (less than 10%). Both stimulator monitoring and the amplified and filtered EMG signal (20,000 times gain, bandwidth from 10 to 1,000 Hz with a notch filter set at 60 Hz) were directed to analog-to-digital converter for recording (Lab-Trax-4, World Precision Instruments, Sarasota, FL) and backup (NI 9215, National Instruments, Austin, TX) and digitized at a sampling rate of 10,000 samples/second. Recordings of the digitized data were made using the software Data Trax2 software (World Precision Instruments) and LabVIEW SignalExpress (National Instruments). A power correlation analysis was used to quantify the correlation between the stimulation pulses of current delivered into the orofacial motor cortex (input signal; µA) and the elicited EMG response in the jaw muscles (output signal; µV). Decrease in the power correlation coefficient (PCC) between these two signals is meant to describe a decrease in the efficacy of the transmission in the neural circuit. Off-line, both signals were rectified and the root mean square (RMS) over each period of the stimulation pulses was calculated in the recorded signals using Data Trax2 software. The transformed data (RMS) from the stimulator monitor and the EMG were then exported with a time resolution of 100 samples/second to a spreadsheet file. The stimulation signal values were used as a reference to select data in a time window of 320 ms starting at the beginning of each train of pulses. This time window was chosen to ensure the analysis of any EMG response whose occurrence or length was delayed from the onset of the stimulation trains and to maximize the exclusion from the analysis of spontaneous jaw movements not associated with the stimulation. Pearson's correlation between the RMS values from the stimulation and EMG signals was then calculated for each experimental subject. PCC was calculated using the data recorded 40 min after the administration of the dose of any compound or vehicle. The effects of the different doses of A$_{2A}$R antagonists on PCC were analyzed by a one-way ANOVA, followed by Dunnett's *post-hoc* test.

In vivo microdialysis

The experiments were performed on freely moving rats 24 h after probe implantation. An artificial cerebrospinal solution of (in mM) 144 NaCl, 4.8 KCl, 1.7 CaCl$_2$, and 1.2 MgCl$_2$ was pumped through the microdialysis probe at a constant rate of 1 µl/min. After a washout period of 90 min, dialysate samples were collected at 20-min intervals. After 60 min of collecting samples for baseline, the rats were injected either with the A$_{2A}$R antagonists KW-6002 or SCH-442416. Both compounds were compared to vehicle controls (5% DMSO, 5% of TWEEN80 and 90% of ddH$_2$O). After 20 min from drug or vehicle injection, electrical stimulation pulses were applied through the electrodes implanted in the orofacial motor cortex for 20 min (pulse of 0.1 ms at 50–150 µA; 100 Hz, 160 ms trains repeating once × second) and samples were collected for 2 additional hours. Glutamate content was measured by reverse-phase HPLC coupled to a flourimetric detector (Shimadzu Inc., Tokio, Japan) [15]. Glutamate values were transformed as percentage of the mean of the three values before the drug or vehicle injection and transformed values were statistically analyzed. The effect of KW-6002, SCH-442416 and vehicle were analyzed using a one-way ANOVA for repeated measures followed by a Tukey's *post-hoc* test.

Cell clones

To obtain CHO cells expressing single receptors or co-expressing A$_{2A}$R and A$_1$R or A$_{2A}$R and D$_2$R, the human cDNAs for A$_1$R or D$_2$R cloned in pcDNA3.1 vector (containing a geneticin resistance gene) were used. The human A$_{2A}$R was cloned into a pcDNA3.1/Hygro vector with a hygromycin resistance gene. For single transfections, CHO cells were transfected with the cDNA corresponding to A$_{2A}$R, A$_1$R or D$_2$R using lipofectamine (Invitrogen, Carlsbad, USA) method following the instructions of the supplier. 24 h after transfection the selection antibiotic was added at a concentration that was previously determined by a selection antibiotic test. Antibiotic resistant clones were isolated in the presence of the selection antibiotic (1200 µg/ml geneticin or

1000 µg/ml hygromycin). After an appropriate number of days/passes, several stable lines were selected and cultured in the presence of the selection antibiotic (600 µg/ml geneticin or 300 µg/ml hygromycin). To obtain clones co-expressing A$_{2A}$R and A$_1$R or A$_{2A}$R and D$_2$R, CHO cells expressing high affinity A$_{2A}$R (obtained as above described) were transfected with the human cDNAs for A$_1$R or D$_2$R cloned in pcDNA3.1 vector using lipofectamine. After an appropriate number of days/passes stable lines were selected and cultured in the presence of the selection antibiotic. The receptor(s) expression in the cell clones was first detected by dot-blot of cell lysates using commercial available antibodies and wild-type CHO cells lysates as negative basal staining. Positively moderated stained clones were grown to obtain membranes in which the receptor expression was quantified by radioligand-binding experiments (see Results).

Bioluminescence Resonance Energy Transfer (BRET) assays

The fusion proteins A$_{2A}$R-*Renilla Luciferase* (A$_{2A}$R-RLuc), A$_1$R-Yellow Fluorescence Protein (A$_1$R-YFP) and D$_2$R-YFP were prepared and characterized as described elsewhere [16]. The cDNA encoding serotonin 5HT$_{2B}$-YFP receptor was kindly provided by Dr. Irma Nardi (University of Pisa, Italy). CHO cells were transiently transfected with the corresponding fusion protein cDNA (see Figure legends) using lipofectamine. Cells were incubated (4 h) with the corresponding cDNA together with lipofectamine and Opti-MEM medium (Invitrogen). After 4 hours, the medium was changed to a fresh complete culture medium. Twenty-four hours after transfection, cells were washed twice in quick succession in HBSS with 10 mM glucose and scraped in 0.5 ml of the same buffer. To control the cell number, sample protein concentration was determined using a Bradford assay kit (Bio-Rad, Munich, Germany) using bovine serum albumin dilutions as standards. To quantify fluorescence proteins, cells (20 µg protein) were distributed in 96-well microplates (black plates with a transparent bottom) and fluorescence was read at 400 nm in a Fluo Star Optima Fluorimeter (BMG Labtechnologies, Offenburg, Germany) equipped with a high-energy xenon flash lamp, using a 10 nm bandwidth excitation filter. Receptor-fluorescence expression was determined as fluorescence of the sample minus the fluorescence of cells expressing protein-Rluc alone. For BRET measurements, the equivalent of 20 µg of cell protein were distributed in 96-well microplates (Corning 3600, white plates; Sigma) and 5 µM coelenterazine H (Molecular Probes, Eugene, OR) was added. After 1 minute of adding coelenterazine H, the readings were collected using a Mithras LB 940, which allows the integration of the signals detected in the 485 nm-short- (440–500 nm) and the 530 nm-long-(510–590 nm) wavelength filters. To quantify receptor-Rluc expression luminescence readings were performed after 10 minutes of adding 5 µM coelenterazine H. The net BRET is defined as [(long-wavelength emission)/(short-wavelength emission)]-Cf where Cf corresponds to [(long-wavelength emission)/(short-wavelength emission)] for the Rluc construct expressed alone in the same experiment.

Radioligand binding experiments

Cells were disrupted with a Polytron homogenizer (PTA 20 TS rotor, setting 3; Kinematica, Basel, Switzerland) for two 5 s-periods in 10 volumes of 50 mM Tris-HCl buffer, pH 7.4 containing a proteinase inhibitor cocktail (Sigma, St. Louis, MO, USA). Cell debris was removed by centrifugation at 1,500 g for 5 min at 4°C and membranes were obtained by centrifugation at 105,000 g (40 min, 4°C). Membranes were resuspended and centrifuged under the same conditions. The pellet was stored at −20°C, washed

once more as described above and resuspended in 50 mM Tris-HCl buffer for immediate use. Membrane protein was quantified by the bicinchoninic acid method (Pierce Chemical Co., Rockford, IL, USA) using bovine serum albumin dilutions as standard. For competition experiments, membrane suspensions (0.2 mg of protein/ml) were incubated for 2 h at 25°C in 50 mM Tris-HCl buffer, pH 7.4, containing 10 mM MgCl$_2$ and 0.2 U/ml of adenosine deaminase (ADA, EC 3.5.4.4; Roche, Basel, Switzerland) with the indicated free concentration of the A$_1$R, A$_{2A}$R, or D$_2$R antagonist [^{3}H]DPCPX (GE Healthcare, UK), [^{3}H]ZM-241385, or [^{3}H]YM-09151-2, respectively (NEN Perkin Elmer, Wellesley, MA, USA) or the A$_1$Ragonist [^{3}H](R)-PIA (Moravek Biochemicals Inc., Brea, CA, USA) and increasing concentrations of DPCPX, ZM-241385, YM-09151-2, the A$_{2A}$R agonist CGS-21680 or the tested A$_{2A}$R antagonist (all provided by CHDI Foundation Inc.). Non-specific binding was determined in the presence of 11 µM of the corresponding non-radiolabelled ligand. Free and membrane-bound ligand were separated by rapid filtration of 500 µl aliquots in a cell harvester (Brandel, Gaithersburg, MD, USA) through Whatman GF/C filters embedded in 0.3% polyethylenimine that were subsequently washed for 5 s with 5 ml of ice-cold 50 mM Tris-HCl buffer. The filters were incubated with 10 ml of Ecoscint H scintillation cocktail (National Diagnostics, Atlanta, GA, USA) overnight at room temperature and radioactivity counts were determined using a Tri-Carb 1600 scintillation counter (PerkinElmer, Boston, MA, USA) with an efficiency of 62% [17]. All displacers were dissolved in DMSO and diluted in the binding medium. The DMSO concentration in the binding incubates was less than 0.5% and, at this concentration, it did not affect agonist or antagonist affinity for their respective receptors.

Binding data analysis

Radioligand competition curves were analyzed by nonlinear regression using the commercial Grafit curve-fitting software (Erithacus Software, Surrey, UK), by fitting the binding data to the mechanistic two-state dimer receptor model [18,19]. Since there is now abundant evidence for GPCR oligomerization, including A$_1$R, A$_{2A}$R and D$_2$R [20–23] and the minimal functional unit of GPCRs in biological tissues seems to imply dimerization [23], this model considers a homodimer as the minimal structural unit of the receptor. Here, we also consider the possibility of a homodimer as the minimal structural unit of a receptor forming homomers or forming heteromers with another receptor. To calculate the macroscopic equilibrium dissociation constants the following equation for a competition binding experiment deduced previously [19,24] was considered:

$$
\begin{aligned}
A_{total\ bound} = & \left(K_{DA2}A + 2A^2 + K_{DA2}AB / K_{DAB} \right) R_T / \\
& \left(K_{DA1}K_{DA2} + K_{DA2}A + A^2 + \right. \\
& K_{DA2}\ AB / K_{DAB} + K_{DA1}K_{DA2}B / K_{DB1} \\
& \left. + K_{DA1}K_{DA2}B^2 / (K_{DB1}K_{DB2}) \right) \\
& + A_{non-specific\ bound}
\end{aligned} \quad (1)
$$

where A represents free radioligand (the adenosine A$_1$R or A$_{2A}$R or dopamine D$_2$R antagonist [^{3}H]DPCPX, [^{3}H]ZM-241385 or [^{3}H]YM-09151-2, respectively or the A$_1$R agonist [^{3}H](R)-PIA) concentration, R$_T$ is the total amount of receptor dimers and K$_{DA1}$ and K$_{DA2}$ are the macroscopic equilibrium dissociation constants describing the binding of the first and the second radioligand molecule (A) to the dimeric receptor; B represents the assayed

competing compound concentration, and K_{DB1} and K_{DB2} are, respectively, the macroscopic equilibrium dissociation constants for the binding of the first ligand molecule (B) to a dimer and for the binding of the second ligand molecule (B) to the semi-occupied dimer; K_{DAB} is the hybrid equilibrium radioligand/competitor dissociation constant, which is the dissociation constant of B binding to a receptor dimer semi-occupied by A.

When the radioligand A shows non-cooperative behaviour, eq. (1) can be simplified to eq. (2) due to the fact that $K_{DA2} = 4K_{DA1}$ [19,25] and, therefore, K_{DA1} is enough to characterize the binding of the radioligand A:

$$A_{total\ bound} = (4K_{DA1}A + 2A^2 + 4K_{DA1}AB / K_{DAB})R_T /$$
$$(4K_{DA1}^2 + 4K_{DA1}A + A^2$$
$$+ 4K_{DA1}AB / K_{DAB} + 4K_{DA1}^2B / K_{DB1} \quad (2)$$
$$+ 4K_{DA1}^2B^2 / (K_{DB1}K_{DB2}))$$
$$+ A_{non-specific\ bound}$$

Binding to GPCRs quite often displays negative cooperativity. Under these circumstances $K_{D2}/K_{D1} > 4$ and then K_{D1} and K_{D2} represent the "high-affinity" and the "low-affinity" binding sites, respectively. On the other hand, for positive cooperativity, $K_{D2}/K_{D1} < 4$ and then K_{D2} represents the "high-affinity" and K_{D1} represents the "low-affinity"binding sites [25]. The two-state dimer model also introduces a cooperativity index (D_{CB}). The dimer cooperativity index for the competing ligand B is calculated as [19,25]:

$$D_{CB} = log\ (4K_{DB1} / K_{DB2})$$

The way the index is defined is such that its value is "0" for non-cooperative binding, positive values of D_C indicate positive cooperativity, whereas negative values imply negative cooperativity [14,19].

In experimental conditions when both the radioligand A and the competitor B (i.e., most adenosine A$_{2A}$ receptor antagonist tested in the present study) show non-cooperativity, it results that $K_{DA2} = 4K_{DA1}$ and $K_{DB2} = 4K_{DB1}$, and eq. (1) can be simplified to:

$$A_{total\ bound} = (4K_{DA1}A + 2A^2 + 4K_{DA1}AB / K_{DAB})\ R_T /$$
$$(4K_{DA1}^2 + 4K_{DA1}A + A^2$$
$$+ 4K_{DA1}\ AB / K_{DAB} + 4K_{DA1}^2B / K_{DB1} \quad (3)$$
$$+ K_{DA1}^2B^2 / K_{DB1}^2) + A_{non-specific\ bound}$$

When both the radioligand A and the competitor B (DPCPX, ZM241385, SCH 23390 or YM-09151-2) are the same compound and the binding is non-cooperative, eq. (3) simplifies to:

$$A_{total\ bound} = (4K_{DA1}A + 2A^2 + AB)R_T /$$
$$(4K_{DA1}^2 + 4K_{DA1}A + A^2$$
$$+ AB + 4K_{DA1}B + B^2) \quad (4)$$
$$+ A_{non-specific\ bound}$$

Goodness of fit was tested according to reduced χ^2 value given by the nonlinear regression program. The test of significance for two different population variances was based upon the F-distribution (see ref. [25] for details). Using this F test, a probability greater than 95% ($p < 0.05$) was considered the criterion to select a more complex equation to fit binding data over the simplest one. In all cases, a probability of less than 70% ($p > 0.30$) resulted when one equation to fit binding data was not significantly better than the other. Results are given as parameter values $\pm$ S.E.M. of three-four independent experiments.

Results

Striatal pre- versus postsynaptic profile of A$_{2A}$ receptor antagonists

Dose-response experiments with the six A$_{2A}$R antagonists indicated that four compounds (SCH-420814, SCH-58261, MSX-3 and ZM-241385) had a similar potency (similar minimal significant effective doses) at inducing locomotor activation (Fig. 1) and at reducing PCC (Fig. 2). The other two compounds had a very different profile: KW-6002 produced a strong locomotor activation already at the dose of 0.3 mg/kg i.p., while it did not reduce PCC at the highest tested dose (10 mg/kg i.p.). On the other hand, SCH-442416 produced a very weak locomotor activation, only significant at doses higher than 3 mg/kg i.p., while it significantly decreased PCC already at the dose of 0.1 mg/kg i.p.

In vivo microdialysis with cortical electrical stimulation was used as an additional in vivo evaluation of the preferential pre- and postsynaptic activity of SCH-442416 and KW-6002, respectively. SCH-442416 significantly counteracted striatal glutamate release induced by cortical stimulation at a dose that strongly reduced PCC but did not induce locomotor activation (1 mg/kg i.p.; Fig. 3). On the other hand, KW-6002 did not modify striatal glutamate release induced by cortical stimulation at a dose that produced a pronounced locomotor activation but did not reduce PCC (1 mg/kg i.p.; Fig. 3).

Development of CHO cell-lines expressing A$_1$-A$_{2A}$ or A$_{2A}$-D$_2$ receptor heteromers

Cell clones expressing A$_{2A}$R, A$_1$R-A$_{2A}$R heteromers or A$_{2A}$R-D$_2$R heteromers and control clones expressing A$_1$R or D$_2$R were generated (see Materials and Methods). First of all, the ability of A$_{2A}$R to form heteromers with A$_1$R or D$_2$R in CHO cells was demonstrated by BRET experiments in cells transiently co-expressing A$_{2A}$R-Rluc and A$_1$R-YFP or A$_{2A}$R-Rluc and D$_2$R-YFP. A positive BRET signal for energy transfer was obtained (Fig. 4). The BRET signal increased as a hyperbolic function of the concentration of the YFP-fusion construct added reaching an asymptote. As a negative control the BRET pair formed by A$_{2A}$R-Rluc and 5-HT$_{2B}$R-YFP was used. As shown in Figure 4, the negative control gave a linear non-specific BRET signal. The significant and hyperbolic BRET signal found for these fusion proteins indicates that the intermolecular interaction between A$_{2A}$R and A$_1$R or A$_{2A}$R and D$_2$R in CHO cells is specific.

A$_{2A}$R-D$_2$R and A$_1$R-A$_{2A}$R heteromerization in stably transfected CHO cells was shown by ligand binding experiments. This is an indirect approach for the identification of a receptor heteromer in native tissues or cells [13]. In the A$_{2A}$R-D$_2$R heteromer, an allosteric interaction between both receptors in the heteromer has been described, in which the dopamine D$_2$R agonist affinity decreases in the presence of an A$_{2A}$R agonist [14]. In CHO cells stably expressing A$_{2A}$R and D$_2$R, the affinity of the D$_2$R for dopamine was determined by competition experiments of the D$_2$R antagonist [³H]YM-09151-2 versus dopamine in the presence (Fig. 5a) or in the absence (Fig. 5b) of the A$_{2A}$R agonist
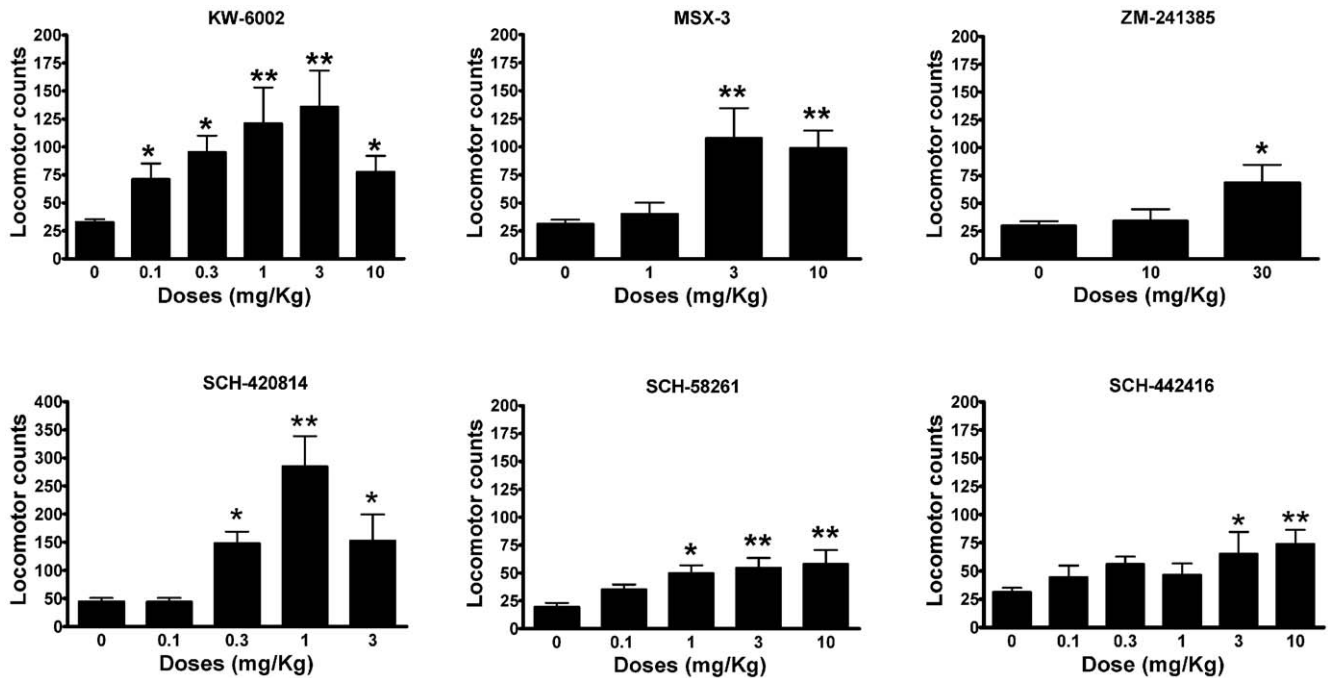
Figure 1. Locomotor activation in rats induced by A$_{2A}$R antagonists. Data represent means $\pm$ S.E.M. of the locomotor activity (distance traveled, in cm, of total accumulated counts) in habituated rats (90 min) during 90 min following the drug administration (n = 6–8 per group). * and **: p<0.05 and p<0.01, respectively in comparison to vehicle-treated animals (0 mg/kg); ANOVA with *post-hoc* Newman–Keuls' comparisons, p<0.5 and p<0.01, respectively).
doi:10.1371/journal.pone.0016088.g001

CGS-21680 (200 nM). By fitting data obtained in the absence of CGS-21680 to eq. 3 (Methods; considering $K_{DA1} = 2.9$ nM see below) the calculated K_{DB1} was 9 ± 2 μM. In the presence of CGS-

21680, 5 μM of dopamine was unable to decrease the radioligand bound and more than 50% of radioligand bound was found in the presence of 100 μM of dopamine (Fig. 5b). A K_{DB1} >30 μM was
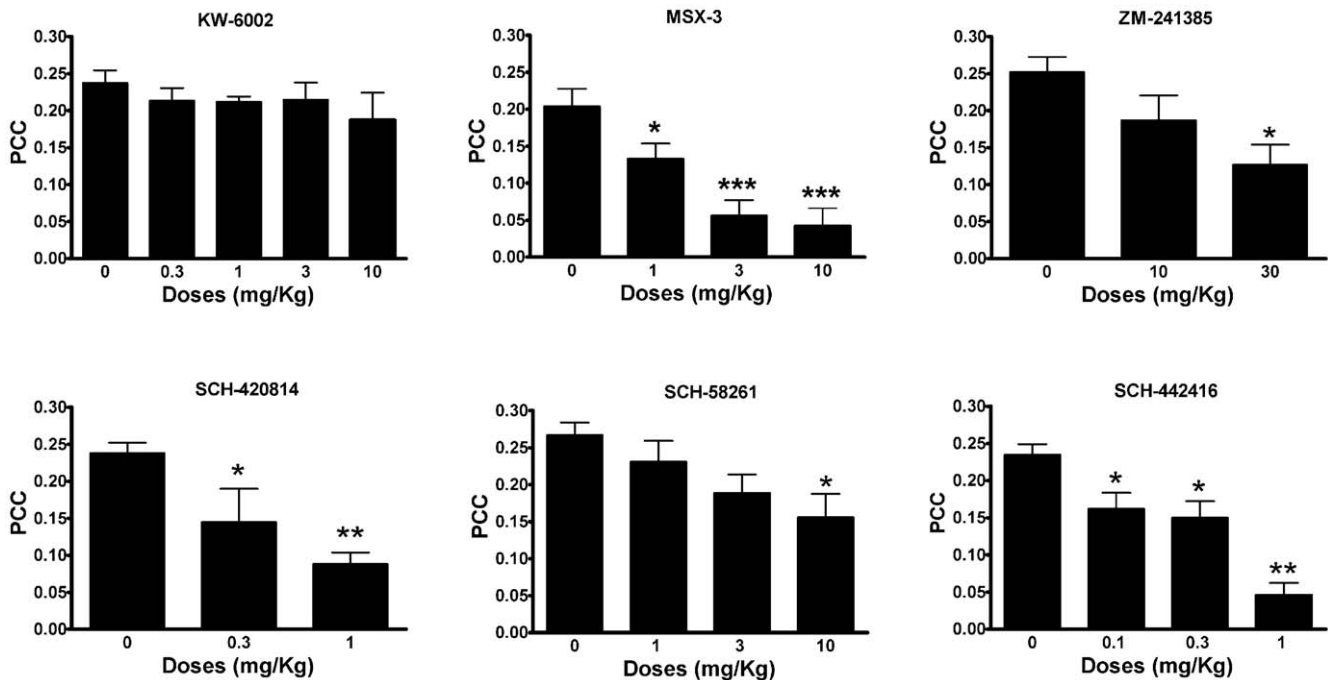

Figure 2. Blockade by A$_{2A}$R antagonists of the motor output induced by cortical electrical stimulation. Dose-dependent decrease in the Power Correlation Coefficient (PCC) induced by the administration of different A$_{2A}$R antagonists. Results represent means $\pm$ S.E.M. (n = 5–6 per group). * and **: p<0.05 and p<0.01, respectively in comparison to vehicle-treated animals (0 mg/kg); ANOVA with *post-hoc* Dunnett' comparisons, p<0.5 and p<0.01, respectively).
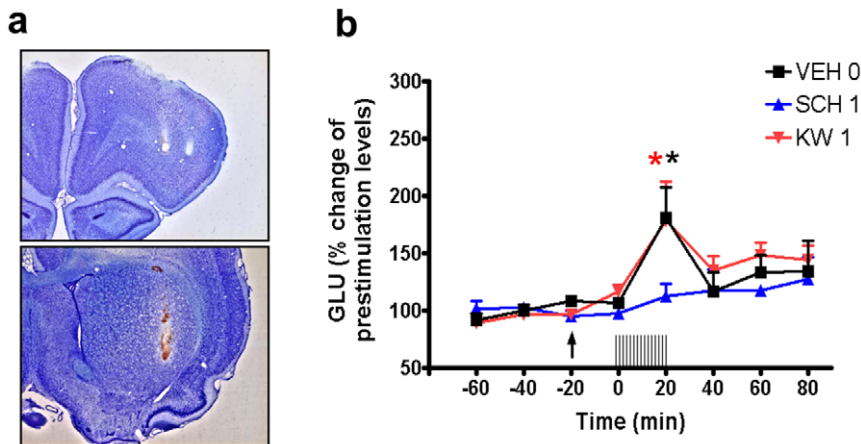doi:10.1371/journal.pone.0016088.g002

Figure 3. Blockade by A$_{2A}$R antagonists of striatal glutamate release induced by cortical electrical stimulation. (a) Representative coronal sections of a rat brain, stained with cresyl violet, showing the tracks left by the bipolar stimulation electrode in the orofacial area of the lateral agranular motor cortex (top) and by the microdialysis probe in the lateral striatum (bottom). (b) Effect of systemic administration of the A$_{2A}$R antagonists SCH-442416 and KW-6002 (1 mg/kg, i.p., in both cases) on the increase in glutamate extracellular levels in the lateral striatum induced by cortical electrical stimulation. Results are expressed as means ± S.E.M. of percentage of the average of the three values before the stimulation (n = 5–7 per group). Time '0' represents the values of the samples previous to the stimulation. The arrow indicates the time of systemic administration. The train of vertical lines represents the period of cortical stimulation. *: $p<0.05$ compared to value of the last sample before the stimulation (repeated-measures ANOVA followed by Tukey's test).
doi:10.1371/journal.pone.0016088.g003

estimated and it was shown that CGS-21680 induced a decrease in the dopamine affinity for D$_2$R. An allosteric interaction in the A$_1$R-A$_{2A}$R heteromer has also been described, in which the A$_1$R agonist affinity decreases in the presence of an A$_{2A}$R agonist [11]. As shown in Figure 6a, the displacement of the A$_1$R agonist [^{3}H]R-PIA by CGS21680 was significantly ($p<0.001$) better fitted by a biphasic than by a monophasic curve. At low CGS-21680 concentrations, when it binds preferentially to A$_{2A}$R (at concentrations of CGS-21680 <500 nM, the direct binding of CGS-21680 to A$_1$R is <1%, according to the calculated affinity of A$_1$R for CGS-21680), CGS-21680 decreased the binding of [^{3}H]R-PIA to the A$_1$R with an IC$_{50}$ value of 386±35 nM (n = 3). At high CGS-21680 concentrations (>10 μM), the [^{3}H]R-PIA binding displacement reflects the binding of CGS-21680 directly to the A$_1$R and the competition between CGS-21680 and R-PIA for the binding to the A$_1$R. In fact, in the control clone expressing only A$_1$R, the displacement by CGS-21680 of [^{3}H]R-PIA only occurred at CGS-21680 concentrations higher than 10 μM (Fig. 6b).

A pharmacological characterization of selected cell clones was performed with competition experiments of radio-labeled antagonists of A$_1$, A$_{2A}$ and D$_2$ receptors versus selective agonists or antagonists. In all cases, the competition curves of the A$_{2A}$R antagonist [^{3}H]ZM-241385 (2 nM) versus ZM-241385 (0.1 nM to 11 μM), the D$_2$R antagonist [^{3}H]YM-09151-2 (0.2 nM) versus YM-09151-2 (0.01 nM to 11 μM) or the A$_1$R antagonist [^{3}H]DPCPX (2 nM) versus DPCPX (0.1 nM to 11 μM), were monophasic, indicating the absence of cooperativity (see Materials and Methods). By fitting the binding data to eq. 4 (Materials and Methods), the K$_D$ (K$_{D1}$) values obtained for the antagonists ZM-241385 or YM-09151-2 were 8±3 nM and 2.9±0.3 nM, respectively, for the chosen A$_{2A}$R-D$_2$R clone, the K$_D$ values obtained for the A$_1$R and A$_{2A}$R antagonists were 8±2 nM (DPCPX) and 1.8±0.4 nM (ZM-241385), respectively, for the chosen A$_1$R-A$_{2A}$R cell clone and the K$_D$ value obtained for A$_{2A}$R antagonist (ZM-241385) was 0.9±0.3 nM for the chosen A$_{2A}$R cell clone. Also by fitting the binding data to eq. 4 (Materials and Methods), the K$_D$ value obtained for the A$_1$R antagonist (DPCPX)

was 8.6±0.9 nM for the A$_1$R cell clone and the K$_D$ value obtained for the D$_2$R antagonist (YM-09151-2) was 0.23±0.08 nM for the D$_2$R cell clone. These values were then used to determine the affinity constants showed in Tables 1 and 2. The agonists affinity in each selected clone was determined by competition experiments using the A$_{2A}$R antagonist [^{3}H]ZM-241385 (2 nM) versus the agonist CGS-21680 (1 nM to 50 μM), the D$_2$R antagonist [^{3}H]YM-09151-2 (0.2 nM), versus the agonist quinpirole (0.1 nM to 30 μM), or the A$_1$R antagonist [^{3}H]DPCPX (2 nM), versus the agonist R-PIA (1 nM to 50 μM). As it is shown in Tables 1 and 2, the agonist affinity for A$_{2A}$R in A$_{2A}$R, A$_{2A}$R-D$_2$R or in A$_{2A}$R-A$_1$R cells is in the same range as that reported for brain striatum or for cells expressing human A$_{2A}$R (between 30 and 250 nM) [7]. Nevertheless, the affinity of the A$_{2A}$R for the selective agonist CGS-21680 was slightly but significantly lower when co-expressed with D$_2$R (see Table 2). A$_1$R (but not A$_{2A}$R or D$_2$R) agonist binding showed negative cooperativity (negative D$_{CB}$ values, see Materials and Methods), both in cells expressing A$_1$R and in cells co-expressing A$_1$R and A$_{2A}$R (Tables 1 and 2).

Screening of A$_{2A}$R antagonists on cells expressing A$_1$-A$_{2A}$ or A$_{2A}$-D$_2$ receptor heteromers

To test if selected A$_{2A}$R antagonists display different selectivity for A$_1$R-A$_{2A}$R or A$_{2A}$R-D$_2$R heteromers, competition experiments with these ligands were performed using CHO cells expressing A$_{2A}$R, A$_1$R-A$_{2A}$R or A$_{2A}$R-D$_2$R. We found that none of the six A$_{2A}$R antagonists first tested in the in vivo models were able to bind with moderate affinity to A$_1$R or to D$_2$R in CHO cells expressing A$_1$R or D$_2$R (data not shown), indicating that these compounds are specific ligands for A$_{2A}$R. Competition experiments of [^{3}H]ZM-241385 (2 nM) binding versus increasing concentrations of each A$_{2A}$R antagonist (1 nM to 100 μM) were performed as indicated in Methods and binding data from competition experiments were fitted assuming that receptors are dimers and statistically (F test, see Materials and Methods) testing whether the competitor (A$_{2A}$R antagonists) binding was cooperative (biphasic competition curves; fitting to eq. 2) or non-cooperative (monophasic competition curves;
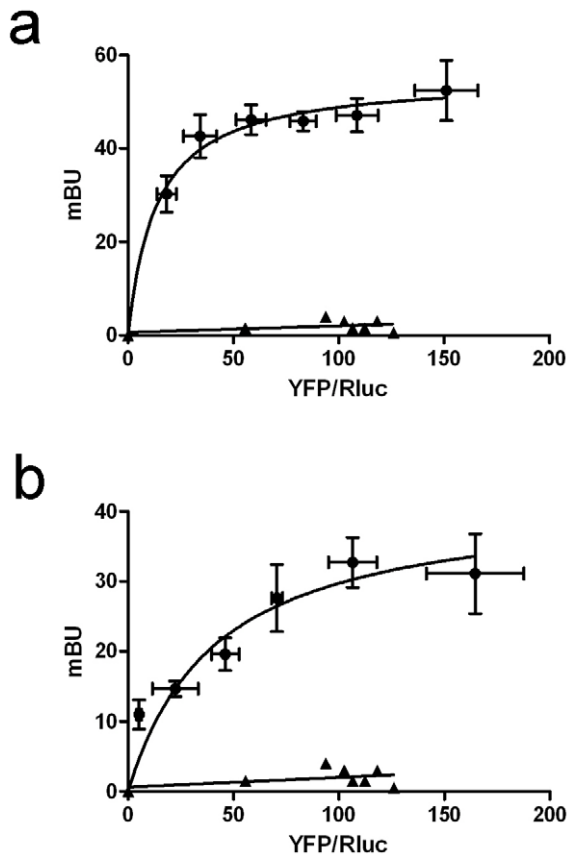
Figure 4. Identification of receptor heteromers in CHO cells by BRET saturation curve. BRET experiments were performed with CHO cells co-expressing A$_{2A}$R-*RLuc* and A$_1$R-YFP (A) or A$_{2A}$R-*RLuc* and D$_2$R-YFP (B). Co-transfections were performed with increasing amounts of plasmid–YFP (0.25 to 4 µg cDNA corresponding to A$_1$R-YFP and 0.5 to 8 µg corresponding to D$_2$R-YFP) whereas the A$_{2A}$R-*RLuc* construct was maintained constant (0.5 µg cDNA). Both fluorescence and luminiscence of each sample were measured before every experiment to confirm similar donor expressions (about 100,000 luminescent units) while monitoring the increase acceptor expression (10,000–25,000 fluorescent units). As a negative control, linear BRET was obtained in cells expressing equivalent luminescence and fluorescence amounts corresponding to A$_{2A}$R-*RLuc*, (0.5 µg transfected cDNA) and serotonin 5HT$_{2B}$-YFP (0.5 to 8 µg transfected cDNA) receptors. The relative amount of acceptor is given as the ratio between the fluorescence of the acceptor minus the fluorescence value of cells expressing the donor alone (YFP) and the luciferase activity of the donor (Rluc). BRET data are expressed as means ± S.D. of 4–6 different experiments grouped as a function of the amount of BRET acceptor.
doi:10.1371/journal.pone.0016088.g004

fitting to eq. 3). Since the screened compounds are A$_{2A}$R antagonists, competition curves were expected to be monophasic, assuming that antagonist binding is not cooperative. In fact, in all cell clones, MSX-2, KW-6002, SCH-420814, ZM-241385 and SCH-58261 gave monophasic competition curves (fitting binding data to eq. 2 was not better than fitting to eq. 3; see Methods and Fig. 7 a–c as an example). Accordingly, the pharmacological characterization for these compounds gave D$_{CB}$ = 0 and K$_{DB2}$ = 4K$_{DB1}$ (see Table 3). For all compounds, co-transfection with A$_1$R did not significantly modify their affinity for A$_{2A}$R. On the other hand, co-transfection with D$_2$R significantly reduced the affinity of A$_{2A}$R for MSX-2, SCH-420814, SCH-58261 and ZM-241385, from two to about nine times, and did not significantly modify the affinity of A$_{2A}$R for KW-6002 (Table 3).
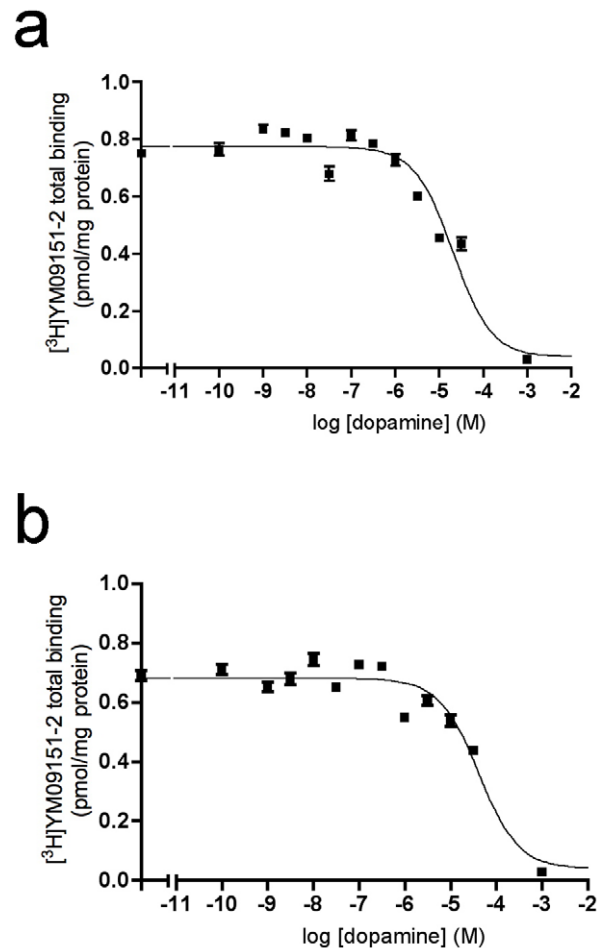

Figure 5. Allosteric interaction between A$_{2A}$R and D$_2$R in A$_{2A}$R-D$_2$R CHO cells. Competition experiments were performed in membrane preparations from CHO cells expressing A$_{2A}$R and D$_2$R with 0.5 nM [^{3}H]YM-09151-2 and increasing concentrations of dopamine (from 0.1 nM to 30 µM) in the absence (a) or in the presence (b) of 200 nM CGS-21680 as indicated in Methods. Data represent means ± S.E.M. of a representative experiment performed with triplicates.
doi:10.1371/journal.pone.0016088.g005

For SCH-442416, a careful statistically-based analysis of the monophasic or biphasic nature of the competition curves led to an unexpected finding: in A$_{2A}$R-D$_2$R cells, competition curves of [^{3}H]ZM-241385 (2 nM) binding *versus* increasing concentrations of SCH-442416 were biphasic (fitting to eq. 2 improves the fitting to eq. 3; see Methods) (Fig. 7d). Table 4 shows the deduced pharmacological parameters from competition experiments of [^{3}H]ZM-241385 *versus* SCH-442416 in cells expressing A$_{2A}$R, A$_1$R-A$_{2A}$R and A$_{2A}$R-D$_2$R. In A$_{2A}$R and A$_1$R-A$_{2A}$R cells the curves were monophasic. Accordingly, the pharmacological characterization gave a D$_{CB}$ values of 0 and a K$_{DB2}$ = 4K$_{DB1}$. In contrast, as mentioned above, in cells expressing A$_{2A}$R-D$_2$R, competition curves were biphasic, and binding data were then fitted to eq. 2 (Methods) and robust parameters were obtained (Table 4). Thus, in A$_{2A}$R-D$_2$R cells, SCH-442416 binding showed a strong negative cooperativity and, consequently, with a marked loss of affinity (an increase of 600 times in K$_{DB2}$) respect to cells expressing A$_{2A}$R. This is reflected by the B$_{50}$ value (concentration competing 50% of radioligand binding), which was more than 40 times higher in A$_{2A}$R-D$_2$R cells than in A$_1$R-A$_{2A}$R cells or A$_{2A}$R cells.
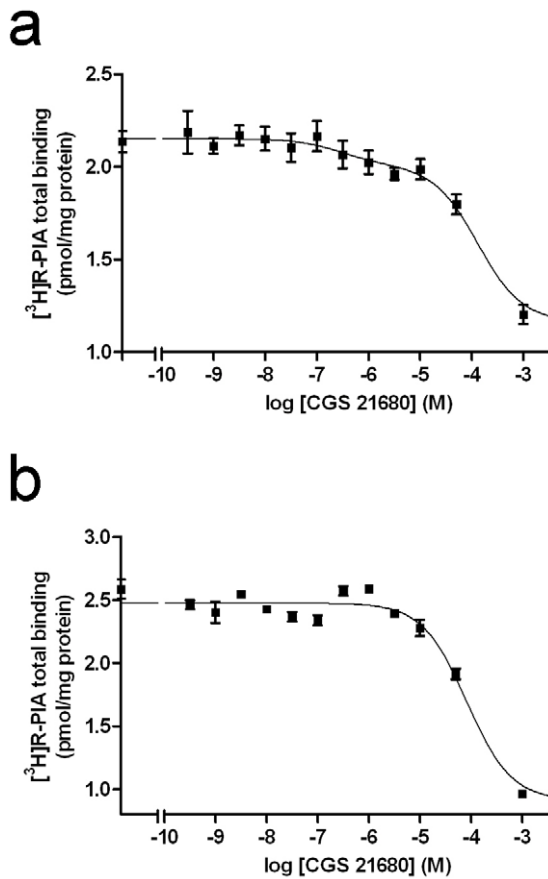
Figure 6. Allosteric interaction between A$_1$R and A$_{2A}$R in A$_1$R-A$_{2A}$R CHO cells. Competition experiments were performed in membrane preparations from CHO cells expressing A$_1$R or A$_1$R and A$_{2A}$R with 12 nM [^{3}H]R-PIA *versus* increasing concentrations of the A$_{2A}$R agonist CGS-21680 as indicated in Methods. Data represent means ± S.E.M. of a representative experiment performed with triplicates.
doi:10.1371/journal.pone.0016088.g006

Discussion

An important finding of the present study is that several A$_{2A}$R antagonists previously thought as being pharmacologically similar present different striatal pre- and postsynaptic profiles. Six compounds already known as selective A$_{2A}$R antagonists were first screened for their ability to block striatal pre- and postsynaptic A$_{2A}$Rs with *in vivo* models. Locomotor activation was used to evaluate postsynaptic activity while PCC reduction was used to determine presynaptic activity (see Introduction). Two compounds, SCH-442416 and KW-6002, showed preferential pre- and postsynaptic profiles, respectively, and four compounds, MSX-3, SCH-420814, SCH-58261 and ZM-241385, showed mixed pre-postsynaptic profiles. Combining *in vivo* microdialysis with cortical electrical stimulation was used as an additional *in vivo* evaluation of presynaptic activity of SCH-442416 and KW-6002. In agreement with its preferential presynaptic profile, SCH-442416 significantly counteracted striatal glutamate release induced by cortical stimulation at a dose (1 mg/kg i.p.) that strongly reduced PCC but did not induce locomotor activation. On the other hand, according to its preferential postsynaptic profile, KW-6002 did not modify striatal glutamate release induced by cortical stimulation at a dose (1 mg/kg i.p.) that produced a pronounced locomotor activation but did not

Table 1. Pharmacological parameters for agonist binding to A$_1$R, A$_{2A}$R and D$_2$R in A$_1$R, A$_{2A}$R and D$_2$R CHO cells.

Parameters	A$_{2A}$R cells	A$_1$R cells	D$_2$R cells
K$_{DB1}$	90±30 nM	13±3 nM	120±60 nM
K$_{DB2}$	360±120 nM	1±0.3 mM	480±240 nM
D$_{CB}$	0	−1.3	0
B$_{50}$	180±60 nM	110±30 nM	240±120 nM

Binding data from competition experiments were fitted assuming that receptors form homodimers, and cooperativity (D$_{CB}$ ≠ 0, fitting to eq. 2; Materials and Methods) or non-cooperativity (D$_{CB}$ = 0, fitting to eq. 3; Materials and Methods) in competitor ligand binding was statistically tested (F test). K$_{DB1}$ and K$_{DB2}$ are, respectively, the equilibrium dissociation constants of the first and second binding of B (the A$_1$R, A$_{2A}$R, or D$_2$R agonists: R-PIA, CGS-21680 or quinpirole, respectively) to the dimer. D$_{CB}$ is the "dimer cooperativity" index for the binding of the ligand B, and B$_{50}$ is the concentration providing half saturation for B. Data are mean ± S.E.M. values of three experiments.
doi:10.1371/journal.pone.0016088.t001

counteract PCC. In a previous study, we reported that intrastriatal perfusion of MSX-3 almost completely counteracted striatal glutamate release induced by cortical electrical stimulation [5], which agrees with its very effective reduction of PCC shown in the present study.

Another important finding of the present study is that at least part of these pharmacological differences between A$_{2A}$R antagonists can be explained by the ability of pre- and postsynaptic A$_{2A}$R to form different receptor heteromers, with A$_1$R and D$_2$R, respectively [4–6,11,14]. Radioligand-binding experiments were performed in CHO cells stably expressing A$_{2A}$R, A$_{2A}$R-D$_2$R heteromers or A$_1$R-A$_{2A}$R heteromers to determine possible differences in the affinity of these compounds for different A$_{2A}$R heteromers. Co-expression with A$_1$R did not significantly modify the affinity of A$_{2A}$R for the different ligands, but co-expression with D$_2$R decreased the affinity of all compounds, with the exception of KW-6002. The structural changes in the A$_{2A}$R induced by heteromerization with the D$_2$R could be detected not only by antagonists but also by agonists. Indeed, the affinity of the selective A$_{2A}$R agonist CGS-21680 was reduced in cells co-

Table 2. Pharmacological parameters for agonist binding to A$_1$R-A$_{2A}$R and A$_{2A}$R-D$_2$R CHO cells.

Parameters	A$_{2A}$R-D$_2$R cells		A$_{2A}$R-A$_1$R cells	
	A$_{2A}$R	D$_2$R	A$_{2A}$R	A$_1$R
K$_{DB1}$	200±40 nM*	1.2±0.6 µM	70±10 nM	0.7±0.3 nM
K$_{DB2}$	0.8±0.4 µM	4.8±2.4 µM	280±40 nM	1.1±0.5 µM
D$_{CB}$	0	0	0	−2.6
B$_{50}$	0.4±0.08 µM	2.4±1.2 µM	140±20 nM	30±10 nM

Binding data from competition experiments were fitted assuming that receptors (also when heteromerizing) form homodimers, and cooperativity (D$_{CB}$ ≠ 0, fitting to eq. 2; Materials and Methods) or non-cooperativity (D$_{CB}$ = 0, fitting to eq. 3; Materials and Methods) in competitor ligand binding was statistically tested (F test). K$_{DB1}$ and K$_{DB2}$ are, respectively, the equilibrium dissociation constants of the first and second binding of B (the A$_1$R, A$_{2A}$R, or D$_2$R agonists: R-PIA, CGS-21680 or quinpirole, respectively) to the dimer. D$_{CB}$ is the "dimer cooperativity" index for the binding of the ligand B, and B$_{50}$ is the concentration providing half saturation for B. Data are mean ± S.E.M. values of three experiments.
*: p<0.05 compared to K$_{DB1}$ values in A$_1$R-A$_{2A}$R and A$_{2A}$R cells (Table 1); one-way ANOVA, followed by Newman-Keuls test.
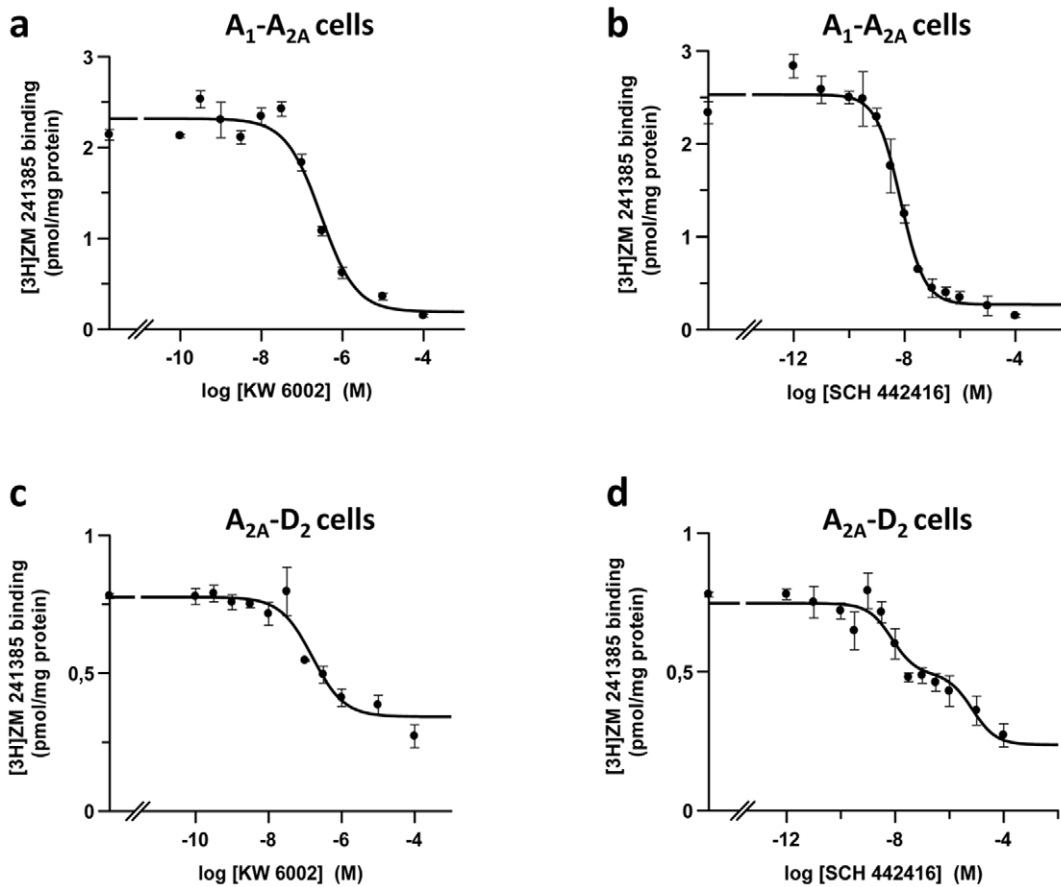doi:10.1371/journal.pone.0016088.t002

Figure 7. Binding of the A$_{2A}$R antagonists KW-6002 and SCH-442416 to A$_1$R-A$_{2A}$R and A$_{2A}$R-D$_2$R CHO cells. Competition experiments of [^{3}H]ZM-241385 (2 nM) *versus* increasing concentrations of KW-6002 (a and c) or SCH-442416 (b and d) were performed as indicated in Methods in membrane preparations from CHO cells expressing A$_1$R and A$_{2A}$R (a and b) or A$_{2A}$R and D$_2$R (c and d). Data are means ± S.E.M. of a representative experiment performed with triplicates.
doi:10.1371/journal.pone.0016088.g007

Table 3. Pharmacological parameters for A$_{2A}$R antagonist binding to A$_{2A}$R, A$_1$R-A$_{2A}$R and A$_{2A}$R-D$_2$R CHO cells.

K$_{D1}$ (nM)	A$_{2A}$R cells	A$_1$R-A$_{2A}$R cells	A$_{2A}$R-D$_2$R cells
ZM241385	0.9±0.3	1.8±0.4	8±3*
SCH58261	3.3±0.3	4.7±0.6	23±8*
MSX2	3.2±0.2	4.2±0.3	7±2*
KW6002	100±10	100±20	160±70
SCH420814	0.5±0.1	1.1±0.1	2.7±0.8*

Competition experiments of [^{3}H]ZM-241385 (2 nM) binding *versus* increasing concentrations of A$_{2A}$ receptor antagonists were performed as indicated in Methods in membrane preparations from CHO cells expressing A$_{2A}$R or A$_1$R and A$_{2A}$R or A$_{2A}$R and D$_2$R. Binding data were fitted assuming that receptors (also when heteromerizing) form homodimers, and cooperativity (D$_{CB}$ ≠ 0, fitting to eq. 2; Materials and Methods) or non-cooperativity (D$_{CB}$ = 0, fitting to eq. 3; Materials and Methods) for competitor ligand binding was statistically tested (F test). Only K$_{DB1}$ values (equilibrium dissociation constant of the first binding of B: ZM-241385, MSX-2, SCH-58261, SCH-420814 or KW-6002) are shown, since the analysis demonstrated non-cooperativity for the five A$_{2A}$R antagonists. Data are mean ± S.E.M. values of three experiments.
*: p<0.05 compared to K$_{DB1}$ values in A$_{2A}$R cells; one-way ANOVA, followed by Newman-Keuls test.
doi:10.1371/journal.pone.0016088.t003

Table 4. Pharmacological parameters for SCH-442416 binding to A$_{2A}$R, A$_1$R-A$_{2A}$R and A$_{2A}$R-D$_2$R CHO cells.

Parameters	A$_{2A}$R cells	A$_1$R-A$_{2A}$R cells	A$_{2A}$R-D$_2$R cells
K$_{DB1}$	2.0±0.3 nM	2.4±0.4 nM	7±4 nM
K$_{DB2}$	8±2 nM	10±2 nM	5±2 µM**
D$_{CB}$	0	0	−2.3
B$_{50}$	4.0±0.6 nM	4.8±0.8 nM	190±80 nM**

Competition experiments of [^{3}H]ZM-241385 (2 nM) binding *versus* increasing concentrations of SCH-442416 were performed as indicated in Methods in membrane preparations from CHO cells expressing A$_{2A}$R or A$_1$R and A$_{2A}$R or A$_{2A}$R and D$_2$R. Results were fitted assuming that receptors (also when heteromerizing) form homodimers, and cooperativity (D$_{CB}$ ≠ 0, fitting to eq. 2; Materials and Methods) or non-cooperativity (D$_{CB}$ = 0, fitting to eq. 3; Materials and Methods) of SCH-442416 binding was statistically tested (F test). K$_{DB1}$ and K$_{DB2}$ are, respectively, the equilibrium dissociation constants of the first and second binding of B (SCH-442416) to the dimer. D$_{CB}$ is the "dimer cooperativity" index for the binding of the ligand B, and B$_{50}$ is the concentration providing half saturation for B. Data are mean ± S.E.M. values of three experiments.
**: p<0.01, respectively compared to the K$_{DB2}$ and B$_{50}$ values in A$_2$R and A$_1$-A$_{2A}$R cells; Kruskal-Wallis, followed by Dunn's test.
doi:10.1371/journal.pone.0016088.t004

transfected with the D$_2$R. When trying to explain the differential action of SCH-442416 observed *in vivo*, it is interesting to note that SCH-442416 showed a much higher affinity for the A$_{2A}$R in a presynaptic-like than in a postsynaptic-like context. The binding of SCH-442416 to the A$_{2A}$R-D$_2$R heteromer displayed a strong negative cooperativity, phenomenon that was not observed for the binding of SCH-442416 to the A$_1$R-A$_{2A}$R heteromer. This negative cooperativity explains the pronounced decrease in affinity of A$_{2A}$R in cells expressing A$_{2A}$R-D$_2$R heteromers (B$_{50}$ values 40 times higher in cells expressing A$_{2A}$R-D$_2$R than A$_1$R-A$_{2A}$R heteromers).

The loss of affinity of A$_{2A}$R upon co-expression of D$_2$R was much less pronounced for ZM-241385, SCH-58261, MSX2 or SCH-420814, for which the affinity was reduced from two to about nine fold. Taking into account that these A$_{2A}$R antagonists behave similarly than the A$_{2A}$R agonist CGS-21680 in terms of binding to A$_1$R-A$_{2A}$R and A$_{2A}$R-D$_2$R heteromers, it is expected that these four compounds compete equally for the binding of the endogenous agonist at pre- and at postsynaptic sites. This would fit with the *in vivo* data, which shows that these compounds have a non-preferred pre-postsynaptic profile. Yet, KW-6002 was the only antagonist whose affinity was not significantly different in cells expressing A$_{2A}$R, A$_1$R-A$_{2A}$R heteromers or A$_{2A}$R-D$_2$R heteromers. Thus, KW-6002 showed the best relative affinity for A$_{2A}$R-D$_2$R heteromers of all coumpounds, which can at least partially explain its preferential postsynaptic profile.

The present results support the notion that receptor heteromers may be used as selective targets for drug development. Main reasons are the very specific neuronal localization of receptor heteromers (even more specific than for receptor subtypes), and a differential ligand affinity of a receptor depending on its partner (or partners) in the receptor heteromer. In the striatum, A$_{2A}$R provides a particularly interesting target, eventually useful for a variety of neuropsychiatric disorders. A$_{2A}$R-D$_2$R and A$_1$R-A$_{2A}$R heteromers are segregated in different striatal neuronal elements. While A$_{2A}$R-D$_2$R heteromers are located postsynaptically in the dendritic spines of the indirect MSNs [4–6,14], A$_1$R-A$_{2A}$R receptor heteromers are located presynaptically in glutamatergic terminals contacting the MSNs of the direct pathway [5,11,14]. Blocking postsynaptic A$_{2A}$R in the indirect MSN should potentiate D$_2$R-mediated motor activation, which is a strategy already used in the development of anti-parkinsonian drugs [26–28]. However, blocking A$_{2A}$R in glutamatergic terminals to the direct MSN could potentially be useful in dyskinetic disorders such as Huntington's disease and maybe in obsessive-compulsive disorders and drug addiction [5]. The present results give a mechanistic explanation to the already reported antiparkinsonian activity of KW-6002 [27,28] and suggest that SCH-442416 could be useful in dyskinetic disorders, obsessive-compulsive disorders and in drug addiction. Medicinal chemistry and computerized modeling should help understanding the molecular properties that determine the particular pharmacological profile of SCH-442416 and KW-6002, which may be used as lead compounds to obtain more effective antidyskinetic and antiparkinsonian compounds, respectively. It will also be of importance to take into account potential changes in the expression of pre- and postsynaptic A$_{2A}$Rs and in their respective heteromers which can occur in those mentioned neuropsychiatric disorders. For instance, dopamine denervation seems to differentially modify the expression of striatal A$_{2A}$R, A$_1$R and D$_2$R [28–31]. This could be addressed by applying the *in vivo* methodology here described to animal models.

Acknowledgments

Author Contributions

Conceived and designed the experiments: MO JB MB CQ VB SRG CL AC RF VC EIC SF. Performed the experiments: MO JB MB CQ AC VC. Analyzed the data: MO CQ CL AC VC SF. Wrote the paper: MO CL AC VC SF.

References

1. Gerfen CR (2004) Basal Ganglia. In: Paxinos G, ed. The Rat Nervous System. Amsterdam: Elsevier Academic Press. pp 445–508.
2. Obeso JA, Rodríguez-Oroz MC, Rodríguez M, Arbizu J, Giménez-Amaya JM (2002) The basal ganglia and disorders of movement: pathophysiological mechanisms. News Physiol Sci 17: 51–55.
3. DeLong MR, Wichmann T (2007) Circuits and circuit disorders of the basal ganglia. Arch Neurol 64: 20–24.
4. Ferre S, Quiroz C, Woods AS, Cunha R, Popoli P, et al. (2008) An update on adenosine A2A-dopamine D2 receptor interactions: Implications for the function of G protein-coupled receptors. Curr Pharm Des 14: 1468–1474.
5. Quiroz C, Lujan R, Uchigashima M, Simoes AP, Lerner TN, et al. (2009) Key Modulatory Role of Presynaptic Adenosine A$_{2A}$ Receptors in Cortical Neurotransmission to the Striatal Direct Pathway. TheScientificWorldJournal 9: 1321–1344.
6. Azdad K, Gall D, Woods AS, Ledent C, Ferré S, et al. (2009) Dopamine D2 and adenosine A2A receptors regulate NMDA-excitation in accumbens neurons through A2A-D2 receptor heteromerization. Neuropsychopharmacology 34: 972–986.
7. Higley MJ, Sabatini BL (2010) Competitive regulation of synaptic Ca2+ influx by D2 dopamine and A2A adenosine receptors. Nat Neurosci 13: 958–966.
8. Svenningsson P, Lindskog M, Ledent C, Parmentier M, Greengard P, et al. (2000) Regulation of the phosphorylation of the dopamine- and cAMP-regulated phosphoprotein of 32 kDa *in vivo* by dopamine D1, dopamine D2, and adenosine A2A receptors. Proc Natl Acad Sci USA 97: 1856–1860.
9. Hakansson K, Galdi S, Hendrick J, Snyder G, Greengard P, et al. (2006) Regulation of phosphorylation of the GluR1 AMPA receptor by dopamine D2 receptors. J Neurochem 96: 482–488.
10. Chen JF, Moratalla R, Impagnatiello F, Grandy DK, Cuellar B, et al. (2001) The role of the D(2) dopamine receptor (D(2)R) in A(2A) adenosine receptor (A(2A)R)-mediated behavioral and cellular responses as revealed by A(2A) and D(2) receptor knockout mice. Proc Natl Acad Sci U S A 98: 1970–1975.
11. Ciruela F, Casadó V, Rodrigues RJ, Luján R, Burgueno J, et al. (2006) Presynaptic control of striatal glutamatergic neurotransmission by adenosine A1-A2A receptor heteromers. J Neurosci 26: 2080–2087.
12. Quiroz C, Pearson V, Gulyani S, Allen R, Earley C, et al. (2010) Up-regulation of striatal A2A receptors with iron deficiency in rats. Effects on locomotion and cortico-striatal neurotransmission. Exp Neurol 224: 292–298.
13. Ferró S, Baler R, Bouvier M, Caron MG, Devi LA, et al. (2009) Building a new conceptual framework for receptor heteromers. Nat Chem Biol 5: 131–134.
14. Ferró S, Ciruela F, Woods AS, Lluis C, Franco R (2007) Functional relevance of neurotransmitter receptor heteromers in the central nervous system. Trends Neurosci 30: 440–446.
15. Quarta D, Ferró S, Solinas M, You Z-B, Hockemeyer J, et al. (2004) Adenosine receptor-mediated modulation of dopamine release in the nucleus accumbens depends on glutamate neurotransmission and NMDA receptor stimulation. J Neurochem 91: 873–880.
16. Navarro G, Aymerich MS, Marcellino D, Cortés A, Casadó V, et al. (2009) Interactions between calmodulin, adenosine A2A and dopamine D2 receptors. J Biol Chem 284: 28058–28068.
17. Sarrió S, Casadó V, Escriche M, Ciruela F, Mallol J, et al. (2000) The heat shock cognate protein hsc73 assembles with A1 adenosine receptors to form functional modules in the cell membrane. Mol Cell Biol 20: 5164–5174.
18. Franco R, Casadó V, Mallol J, Ferró S, Fuxe K, et al. (2005) Dimer-based model for heptaspanning membrana receptors. Trends Biochem Sci 26: 221–232.
19. Casadó V, Cortés A, Mallol J, Pérez-Capote K, Ferró S, et al. (2009) GPCR homomers and heteromers: A better choice as targets for drug development than GPCR monomers? Pharmacol Ther 124: 248–257.
20. Ciruela F, Casadó V, Mallol J, Canela EI, Lluis C, et al. (1995) Immunological identification of A1 adenosine receptors in brain cortex. J Neurosci Res 42: 818–828.
21. Canals M, Burgueño J, Marcellino D, Cabello N, Canela EI, et al. (2004) Homodimerization of adenosine A2A receptors: qualitative and quantitative

assessment by fluorescence and bioluminescence energy transfer. J Neurochem 88: 726–734.

22. Guo W, Urizar E, Kralikova M, Mobarec JC, Shi L, et al. (2008) Dopamine D2 receptors form higher order oligomers at physiological expresión levels. EMBO J 27: 2293–2304.

23. Han Y, Moreira IS, Urizar E, Weinstein H, Javitch JA (2009) Allosteric Communications between protomers of dopamine class A GPCR dimers modulates activation. Nat Chem Biol 9: 688–695.

24. Casadó V, Cortes A, Ciruela F, Mallol J, et al. (2007) Old and new ways to calculate the affinity of agonists and antagonists interacting with G-protein-coupled monomeric and dimeric receptors: The receptor-dimer cooperativity index. Pharmacol Ther 116: 343–354.

25. Casadó V, Martí T, Franco R, Lluis C, Mallol J, et al. (1990) A method for binding parameters estimation of A1 adenosine receptor subtype: a practical approach. Anal Biochem 184: 117–123.

26. Schwarzschild MA, Agnati L, Fuxe K, Chen JF, Morelli M (2007) Targeting adenosine A2A receptors in Parkinson's disease Trends Neurosci 29: 647–654.

27. Jenner P (2003) A2A antagonists as novel non-dopaminergic therapy for motor dysfunction in PD Neurology 61: S32–S8.

28. Stacy M, Silver D, Mendis T, Sutton J, Mori A, et al. (2008) A 12-week, placebo-controlled study (6002-US-006) of istradefylline in Parkinson disease Neurology 70: 2233–2240.

29. Kaasinen V, Ruottinen HM, Någren K, Lehikoinen P, Oikonen V, et al. (2000) Upregulation of putaminal dopamine D2 receptors in early Parkinson's disease: a comparative PET study with [11C] raclopride and [11C]N-methylspiperone J Nucl Med 41: 65–70.

30. Pinna A, Corsi C, Carta AR, Valentini V, Pedata F, et al. (2002) Modification of adenosine extracellular levels and adenosine A(2A) receptor mRNA by dopamine denervation. Eur J Pharmacol 446: 75–82.

31. Varani K, Vincenzi F, Tosi A, Gessi S, Casetta I, et al. (2010) A2A adenosine receptor overexpression and functionality, as well as TNF-alpha levels, correlate with motor symptoms in Parkinson's disease FASEB J 24: 587–598.